



Acoustic emission characteristics of different brittle rocks and its application in brittleness evaluation

Hui Zhang · Zhizhang Wang · Zhenlong Song  · Yuzhu Zhang · Tingting wang · Wanchun Zhao

Received: 2 January 2021 / Accepted: 15 April 2021 / Published online: 4 May 2021
© The Author(s), under exclusive licence to Springer Nature Switzerland AG 2021

Abstract Rock brittleness is an essential factor affecting underground engineering disasters and energy extraction. A large number of cracks are generated during rock destruction, and many acoustic emission (AE) signals are accompanied. The propagation speed and modes of cracks in different brittle rocks differ during failure, and their AE signals also show differing characteristics. In this study, uniaxial compression experiments cooperating with AE monitoring on rock-like materials with different brittleness were conducted. We found that as the rock brittleness increased, the AE energy increased sharply during loading. During rock failure, the proportion of AE signals with lower RA (rise time/amplitude) and higher AF (average frequency) increased as rock brittleness increased. Based on the experimental

results, the AE parameter ib_E -value was proposed to evaluate the crack propagation state of the rocks. This ib_E -value is also a parameter that determines the crack initiation point and residual stress point. Based on the variation characteristic of the ib_E -value during the rock failure process and the first pressure drop after the peak of the rock, two evaluation criteria for rock brittleness were proposed. Compared with other brittleness evaluation criteria, these two evaluation criteria have better discrimination for different brittleness rocks, guiding human underground resource extraction and engineering disaster prevention.

Article highlights

1. At the moment of rock failure, the proportion of AE with lower RA and higher AF increases gradually with the increase of rock brittleness.
2. Based on the Gutenberg and Richter, we propose an AE index ib_E -value, which can reflect the rock's crack propagation state.
3. Based on ib_E -value, we propose a brittleness index, which has higher sensitivity and reliability than other brittleness indexes.

H. Zhang · Z. Wang
College of Geosciences, China University of Petroleum,
Beijing 102249, China

H. Zhang
PetroChina Jilin Oilfield Company, Songyuan 138000,
Jilin, China

Z. Song (✉) · T. wang · W. Zhao
Northeast Petroleum University, Daqing 163318,
Heilongjiang, China
e-mail: zhenlongsong@cqu.edu.cn

Y. Zhang
China Coal Technology and Engineering Group
Chongqing Research Institute, Chongqing 400037, China

Keywords Brittleness index · Acoustic emission · Fracture propagation · ib_E -Value

1 Introduction

Rock brittleness has a significant effect on the rock failure morphology. Under high-stress conditions, brittle rocks are prone to underground engineering disasters such as rock bursts (Gong et al. 2019). Many scholars have proposed several evaluation indices for rock burst proneness (Song et al. 2015; Gong et al. 2018). Some scholars also researched the brittle behavior of intact rock (Munoz et al. 2016a; Zhang et al. 2018b) and jointed rock (Li et al. 2019a, b, c; Yang et al. 2019) during disasters. The quantitative description of rock brittleness is of great significance for underground resource extraction (oil extraction, geothermal exploitation, shale gas extraction, etc.; Li et al. 2018). Wanniarachchi et al. (2015) found that cracks were more likely to initiate and propagate in brittle shale and that more energy was needed to deform in more ductile shale. In order to quantitatively characterize the brittleness of rocks, many brittleness indexes (shown in Table 1) have been proposed (Li et al. 2019c; Wang et al. 2020). Some scholars have comprehensively considered the relationship between stress and strain, and use Young's modulus and Poisson's ratio to evaluate the brittleness of rocks. Scholars also found that the higher the Young's modulus, the greater the increase in rock brittleness (Turcotte et al. 2003; Carpinteri and Lacidogna 2006).

Brittle rocks had high elastic modulus and low Poisson's ratio (Jahandideh and Jafarpour 2016); that is, they had a high shear model ($G = E/(2*(1 + \nu))$, where G is the shear modulus, and E and ν are Young's modulus and Poisson's ratio), which was also confirmed by Grieser and Bray (2007). These studies have shown that brittle rocks are a sudden failure under small strain conditions and that brittle rocks suddenly rupture with crack propagation and produce a large stress drop within small plastic deformations (Feng et al. 2016). These brittleness indicators use pre-peak strength parameters (e.g., elastic modulus and Poisson's ratio) that do not fully reflect the entire loading process of the rock and are therefore only applicable to brittle rocks. Other scholars have evaluated the brittleness of rock in response to the energy change during rock failure. Tarasov and Potvin (2013) conducted a series of triaxial compression experiments, based on which two brittleness indicators considering the energy balance of the rock mass in the post-peak were proposed. Munoz et al. (2016b) used clever loading methods to obtain a complete stress-strain, including class I and class II behavior and developed a brittleness index based on fracture energy dissipation. Although scholars have put forward many quantitative indicators of brittleness, most of the brittleness criteria are based on traditional stress-strain curves, lacking characterization of microscopic changes within rocks.

Table 1 Summary of brittleness index definitions cited in this paper

Formula	Variable description	Test method	References
$BI_1 = \frac{Q}{Q+C+Cl}$	Q : quartz;	Mineralogical logging	Jarvie et al. (2007)
$BI_2 = \frac{Q + Dol}{Q + Dol + Lm + Cl + TOC}$	C : carbonate; Cl : clay; Dol : dolomite; Lm : limestone; TOC : total organic content		
$BI_3 = \frac{M-E}{M}$	E is the unloading elastic modulus;	Stress strain test	Tarasov and Potvin (2013)
$BI_4 = \frac{E}{M}$	M is the post-peak elastic modulus		
$BI_5 = \frac{U_e}{U_{total}}$	U_e is the elastic energy;		Munoz et al. (2016b)
$BI_6 = \frac{U_e}{U_{post}}$	U_{total} is the total fracture energy;		
$BI_7 = \frac{U_{peak}}{U_{total}}$	U_{peak} is the strain energy until peak stress; U_{post} is energy include post-peak		
$IB_8 = \frac{\tau_p - \tau_r}{\tau_p}$	τ_p represents the shear force at the peak τ_r represents the residual shear stress		Bishop (1967)

However, the entire process of rock failure involves microscopic damage to the rock, where microcracks emerge, propagate, and eventually form macro-cracks, leading to rock destruction. The study of crack energy during rock failure can help us better understand the brittleness of rocks.

Acoustic emission (AE), as a commonly used nondestructive testing technique, can effectively detect the fracture process inside the rock (Yang et al. 2021). Attempts have also been made to use AE to measure the brittleness of rocks. Parney and Lange (2010) used AE to calculate Young's modulus and Poisson's ratio of rocks using P-wave and S-wave and then estimated the brittleness with Young's modulus and Poisson's ratio. Perez and Marfurt (2013) used micro-vibration events to evaluate the brittleness of shale. Duan et al. (2020) found a good correspondence between the development of cracks in rocks and AE. However, few reports are on the analysis of the AE characteristics of brittle rock and the use of AE waveforms to evaluate rock brittleness. The AE waveform contains almost the entire process of crack propagation. Zhang et al. (2018a, b) found that the uniaxial compression process can be divided into three stages: the AE silent stage, the slow rising stage, and the rapid rising stage. Li et al. (2019a, b, c) also found that rocks have different AE characteristics at different loading stages. The AE activity of rocks before failure will increase significantly, and the amplitude of the increase is also closely related to the characteristics of the rocks. The values of AE parameters RA and AF (average frequency) are determined by the proportion of tensile and shear cracks during rock failure (Grosse and Ohtsu 2008), and the RA–AF ratio is used to evaluate and analyze different materials (Ohtsu 2011). Mansurov (1994) predicted the type of rock failure based on the AE phenomenon of the destruction process. At the same time, scholars believe that rock fractures and earthquakes have similar statistical laws. Schiavi et al. (2011) performed uniaxial compression experiments on brittle concrete materials and found that the b -value of the samples would decrease before failure. Chen et al. (2021) mentioned a possible potential link between b -value and brittleness. Based on the b -value, Shiotani et al. (1994) described the expansion law of rock cracks and found that different ib -values (improved b value) of the same rock represented different sizes of crack propagation (Kurz et al. 2006). AE can reflect the change in energy inside

the rock. Using the ib -values method to count AE energy to quantify the rock brittleness has certain advantages over traditional quantitative expression methods.

Based on the above analysis, this study carried out uniaxial loading tests of different brittle materials and recorded the AE waveforms during the loading process. A rock brittleness index based on the characteristics of energy release during rock failure is proposed using the statistical method of ib -values, which provides a feasible method for brittleness evaluation in engineering practice.

2 Materials and methods

In order to study the AE laws of different brittle rocks, uniaxial failure experiments were performed with different brittle rock-like materials, and the AE signals generated by the samples during loading were recorded. Some scholars believe that the difference in rock brittleness is caused by the mineral composition and composition of the rock. Rickman et al. (2008) analyzed the mineral composition of the Barnett shale by dividing the mineral composition of the shale into quartz minerals, carbonate minerals, and clay minerals. It was also noted that with the increase in quartz mineral content, the brittleness index of shale increased (Jarvie et al. 2007; Wang and Gale 2009). Therefore, combined with the actual mineral composition parameters of the reservoir rock layer, engineering sand, quartz, clay minerals, cement were selected. The water-to-material ratio of the specimen is 1:2.5, and the water and material are fully mixed by a mixer to eliminate the heterogeneity of the specimens. The brittle mineral contents (the ratio of engineering sand to quartz is 1:1) were prepared according to the mineral composition: 0%, 10%, 30%, and 50% of similar brittle samples with different brittleness (numbered 1[#], 2[#], 3[#], and 4[#], respectively) and square samples with dimensions of 50 mm × 50 mm × 50 mm. In this experiment, a WSM-200kN microcomputer control loading system (Fig. 1) was used to conduct uniaxial compression tests using the displacement control method at a 2 mm/min loading rate. We used the American Physical Acoustics Corporation (PAC) AE system. The parameters of the AE workstation were shown in Table 2. Nano-30 ceramic-surface AE sensors (produced by PAC) with a

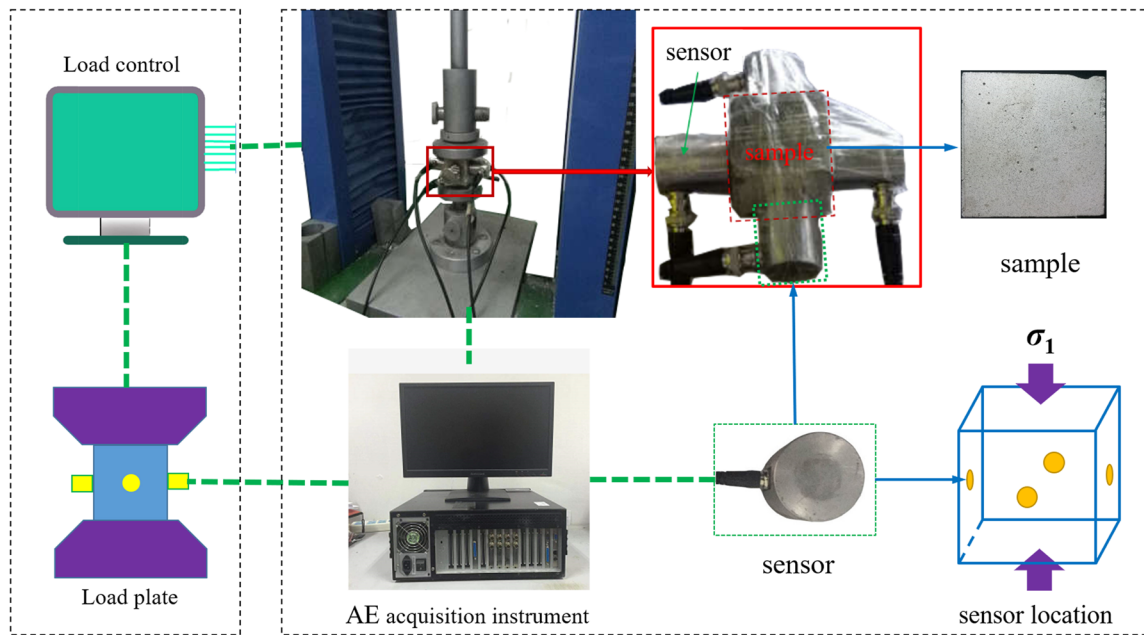


Fig. 1 WSM-200kN microcomputer control loading system and AE monitoring system

Table 2 The parameters of DISP series AE workstation

Capability index	Value
Quantity of channels	12
Resolution (dB)	1
Maximum sampling rate (MSPS)	40
Minimum noise threshold (dB)	22
Frequency response (kHz)	$1.0 \sim 3 \times 10^3$

good frequency response in the range of 125–750 kHz were installed on the specimen. In this experiment, we used four channels to collect data with a threshold of 40 dB, a preamplifier gain of 40 dB, and a sampling frequency of 1 MHz. The AE signals transmission efficiency can be improved by applying a coupling agent between the sample and the AE sensors to exhaust the air in the contact surface between them. The upper and lower sides of the specimen need to be loaded, and four AE sensors were placed in the center of the four sides of the sample (Fig. 1). Since this experiment is to collect waveform signals, not to locate the AE events, a larger sensor is selected to receive more internal rupture signals. In order to reduce the end effect and vibration of the press on the

AE signal, a 50 mm square rubber sheet was placed at both ends of the samples.

3 Experiment results

3.1 The energy and hits character of AE for different brittle rock

The energy and hit are important for representing the crack state during rock failure. Figure 2 shows the characteristics of the AE energy and hits during the failure of different brittle rocks. As the brittleness of the rock increases, the strength of the rock gradually increases to approximately 27 MPa. With the increasing of loading stress, the cumulative energy of the AE generated by low-brittle samples (e.g., samples 1[#] and 2[#]) increased slowly. The rising-rate increased during the failure stage, and the AE counts (AE hits) in the strain interval are also slowly rising, but the overall difference is not very significant. Compared with brittle samples (samples 3[#] and 4[#]), in the elastic stage (Fig. 2c). The energy of brittle samples rises stepwise, and the internally released energy is a pulse-type (Fig. 2d), which also reflects the suddenness of internal failure of the brittle rock. The total AE energy released from sample 4[#] at rock failure is not the

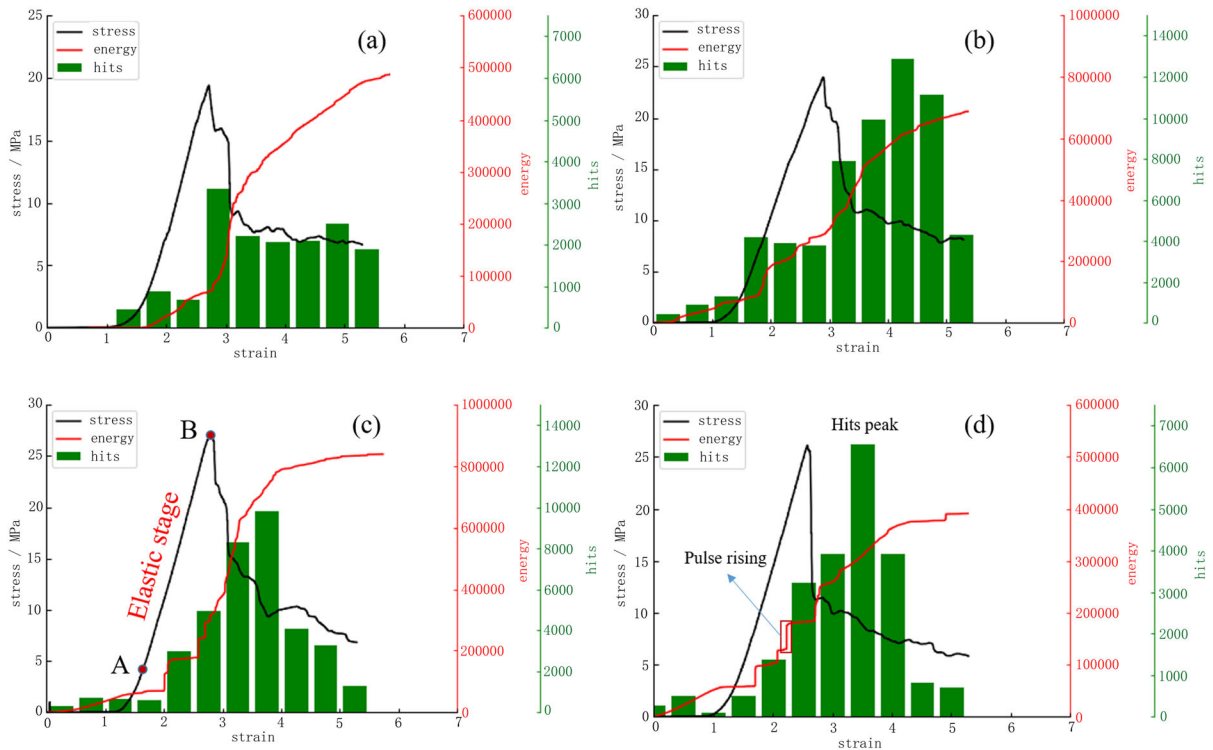


Fig. 2 The relationship between stress–strain and the AE hits and energy

highest, but the rising rate is substantial. At the same time, it is observed that the hit value increases and then decreases during loading. The brittle sample had more hits after the first pressure drop. In other words, there were not many hits before the peak. This phenomenon may be related to the failure modes of different brittle materials. In order to analyze the failure process and failure mode inside the material more clearly, RA–AF parameters are introduced in this paper.

3.2 The RA–AF characters of different brittle rock

The AF value and RA value usually evaluate the crack type in geo-material engineering (Aggelis et al. 2012). The classification principles and criteria are shown in Fig. 3. The RA value is the ratio of the rise time to the maximum amplitude, and the smaller the value, the faster the power of the AE waveform rises. The AF value is the average frequency of the AE wave. It is generally believed that tensile fractures have low RA values and high AF values, and many scholars extensively using this principle to classify crack types (Lin et al. 2018).

Therefore, we can judge the fracture of different brittle rocks according to the distribution of RA and AF in the failure process. The distribution of cracks and fractures of different brittle rocks were analyzed more clearly by the distribution characteristics of RA and AF at the moment of rock failure (Fig. 4).

According to the theory of Aggelis (2011), shear cracks always generate AE waves with low AF. The RA value can reflect the fracture modes (Stankevych and Skalsky 2016), indicating that the fracture modes differ from the change in brittleness. In order to more clearly show the distribution law of the AE generated by different brittle rocks in the RA–AF diagram, we have carried out quantitative statistics on the number of AE of different brittle rocks according to the RA value and AF value. The statistical results are shown in Fig. 4, where the color indicates the distribution of the AE number within the RA–AF range. Figure 4 shows that as the brittleness of the rock increases, the distribution ratio of the AE generated by the rock in low AF and high RA gradually decreases. For the weakest rock sample #1, the distribution of AE in low AF (AF less than 10) and high RA (RA more than 102)

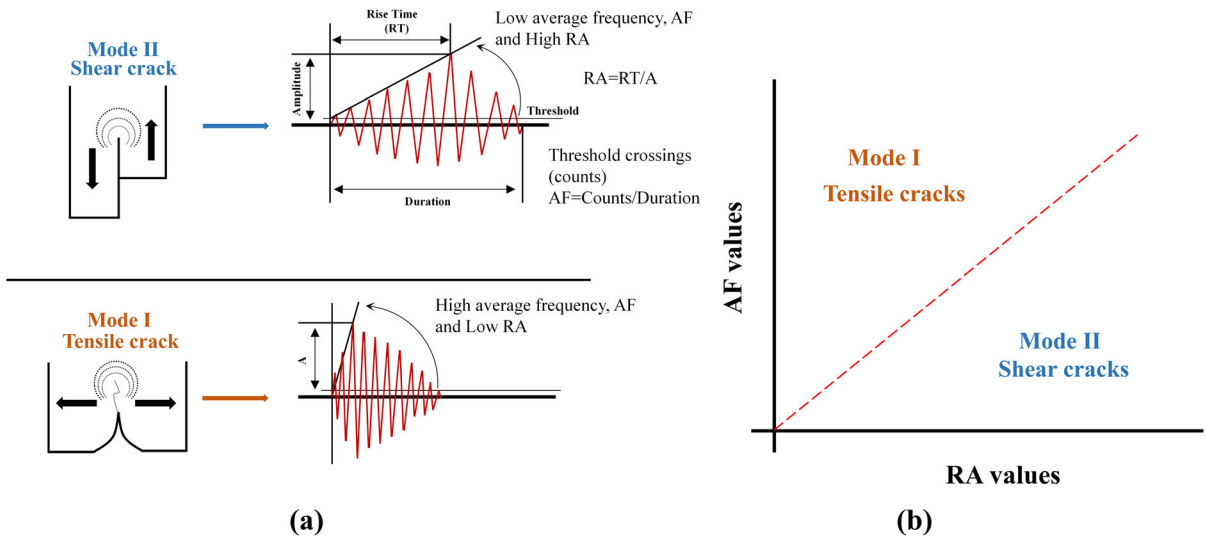


Fig. 3 Crack classification method based on the waveform principle. **a** Waveform principle, **b** crack classification method

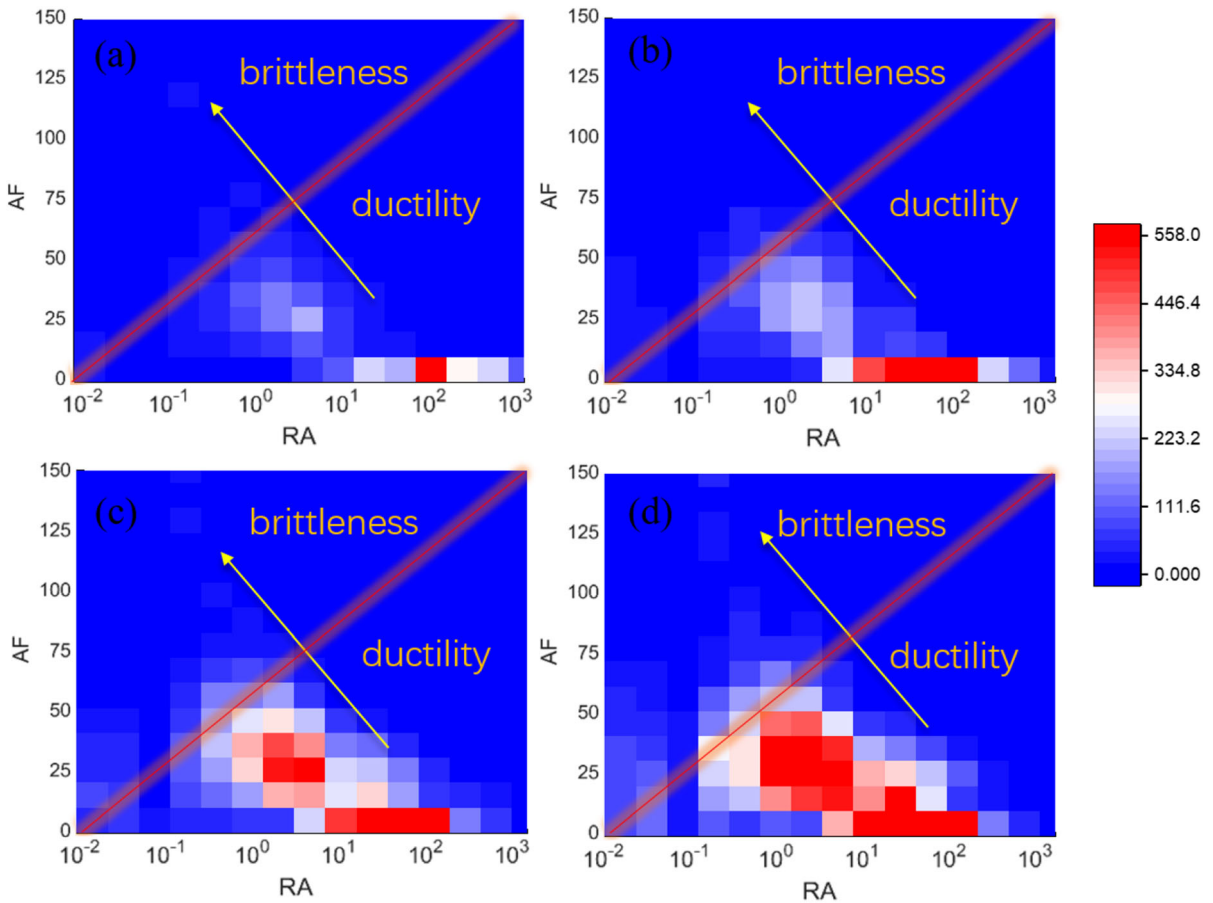


Fig. 4 RA–AF distribution of acoustic emission in different brittleness rocks. The brittleness of **a–d** specimens increases successively

is 27.6%. With the increase of rock brittleness, the proportions of #2, #3 and #4 specimens in this area gradually decrease, which are 18.4%, 16.5% and 5.3%, respectively.

According to the theory of Aggelis (2011), a classification benchmark line has been added to the RA–AF diagram. It should be noted here that this line is not a strict dividing line between tensile cracks and shear cracks, but rather a baseline for determining the ratio of tensile cracks and shear cracks. As the brittleness increases, the number of AE at the classification benchmark line (AF is between 20–40 and RA is between 0.1–1) changes particularly significantly. With the increase of brittleness, the area gradually changes from weakly brittle white to red, which indicates that the distribution of AE in RA–AF is becoming more and more uniform. For example, the number of AE in this area of specimen 1# with the weakest brittleness is 960. With the increase of brittleness, the number of AE of specimens #2, #3 and #4 in this area were 1127, 2639 and 4136, respectively. These AE distribution characteristics indicate that as the brittleness of the rock increases, more tensile signals are generated during rock fracture. In addition, the energy of tensile AE is often lower, so the number of tensile AEs generated per unit of energy is more than that of shear, and this may be why the total amount of AE increases with the increase of brittleness.

3.3 The variation characteristics of AE energy during the fracture of brittle rocks

(1) The ib_E -value

The brittleness rock is a process of high-speed release of the rock's internal strain energy during failure (Zhang et al., 2016). Most of the energy of the brittle rock is stored in the form of strain energy during loading, and the energy is released to crack propagation during failure. Therefore, the brittleness of the rock can be considered a characteristic of strain energy release during loading and failure, meaning that the brittleness of the rock can be transformed into the problem of the strain energy release power and form. As mentioned in many experiments, there is little plastic deformation and microcrack initiation in high brittle rock during loading as high modulus and low Poisson's ratio are maintained (Jahandideh and

Jafarpour 2016). The ductility rock slowly releases strain energy in the form of plastic deformation during loading. Both the plastic deformation and the microcrack propagation of the rock will generate AEs (Grosse and Ohtsu 2008). Therefore, for rock crack propagation, the AE characteristics of rock during loading can be used as an index of rock brittleness. In this paper, we proposed the ib_E -value to show the variation characteristics of AE energy based on the statistical method of Shiotani et al. (1994) and the b_E parameter of Sagasta et al. (2018).

Although there are significant differences between rock fractures and earthquakes in geometric scale, time scale, and boundary conditions, there are similar statistical laws between them (Hirata 1987; Garcimartín et al. 1997). In earthquakes, scholars use b -values to describe the law of fractures between plates. Scholars refer to the relationship between earthquake magnitude and frequency (G–R relationship) proposed by Gutenberg and Richter (1945) to measure the rock failure process. Sagasta proposed the energy- b -value (b_E -value) parameter describing the degree of rock failure:

$$\text{Log}_{10}N(\text{AEE}) = a - b_E \text{Log}_{10}(\text{AEE}) \quad (1)$$

where AEE represents the energy of the AE event, $N(\text{AEE})$ is the accumulated number of AE events with energy not less than AEE, and a and b_E are constants.

This expression indicates that $N(\text{AEE})$ decreases exponentially with an increase in the magnitude of energy. The reduced slope coefficient b_E can be used to measure the crack propagation in the rock. According to the definition of the energy b_E -value, statistical calculations were performed on the AE data of the samples (Fig. 5). From Fig. 5, we found a good linear relationship between the AE events and AE energy in the area where the AE energy was 10 to 10,000 aJ (1 aJ = 10^{-18} Joules). However, the predicted b_E -value is lower when the AE energy is small, and the b_E -value is higher when the $\log(\text{AEE})$ is larger. Therefore, the statistics of all data will seriously affect the accuracy of the statistical results. There are many differences between AE and earthquakes. In the earthquake, a large number of low-energy rupture signals could not be recorded. Thus, we cannot directly apply the b -value calculation method in the earthquake to deal with AE data, and statistical evaluation of the generated AE data is required before the evaluation.

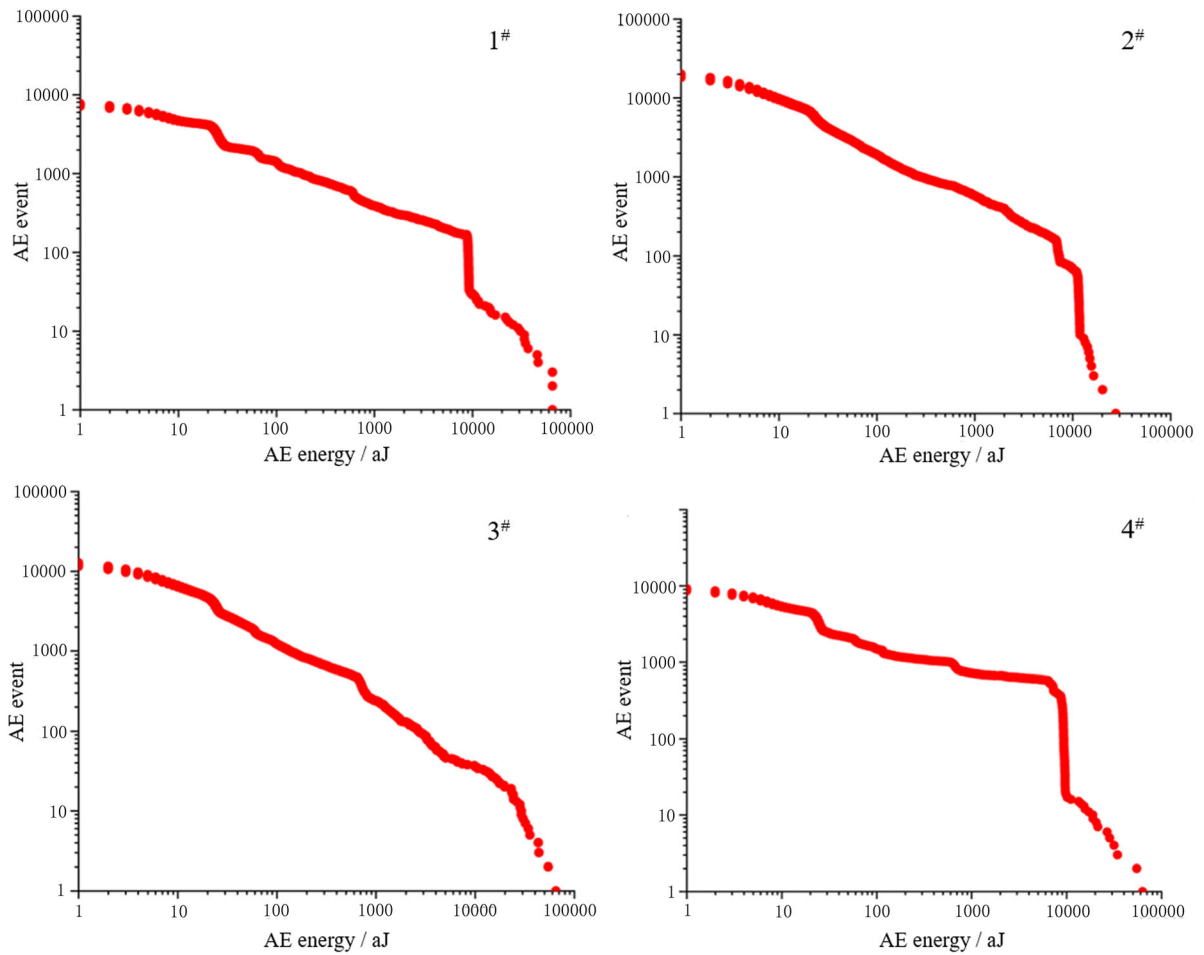


Fig. 5 The b_E -value statistics in the experiment. This is the calculated result of b_E -value.

In order to accurately reflect the energy changes of AE during rock failure, we selected a series of AE data β (the value of β is generally 50–100) according to the distribution characteristics of AE events. Among these events, only the signals with exceeding amplitudes $\mu - \alpha_1\sigma$ were selected to calculate the ib_E -value. This method can effectively remove micro energy events and avoid the influence of many low-energy AE events on the calculation results (Shiotani et al. 1994). The ib_E value is calculated as follows:

$$ib_E = \frac{\log_{10} N(w_1) - \log_{10} N(w_2)}{(\alpha_1 + \alpha_2)\sigma} \tag{2}$$

That is $N(w_1)$ and $N(w_2)$ in formula (2) denote the amount of energy exceeding $\mu - \alpha_1\sigma$ and $\mu + \alpha_2\sigma$, respectively, and α_1 and α_2 are taken as 0 and 1 (Shiotani et al. 2001a; Colombo et al. 2003; Watanabe

et al. 2007). We test this method with the experimental data in this paper.

Figure 6 shows the change in the ib_E value during the full stress–strain process. When the brittleness is weak (sample 1[#]), the ib_E value is kept at a low level. As brittleness increases, the ib_E value produced during the elastic loading stage first increase and then decrease. The ib_E of sample 4[#] with high brittleness is always at a low level in the elastic loading stage, and a noticeable ib_E value drop appears in the failure stage. In the post-peak phase, each pressure drop corresponds to a decrease in the ib_E -value. Especially in experiment 4[#], the peak point and lowest point of the ib_E -value correspond to the peak point of the rock stress and first pressure drop point, respectively. Many scholars have analyzed the failure process of rock with b -value and ib -value and concluded that these values

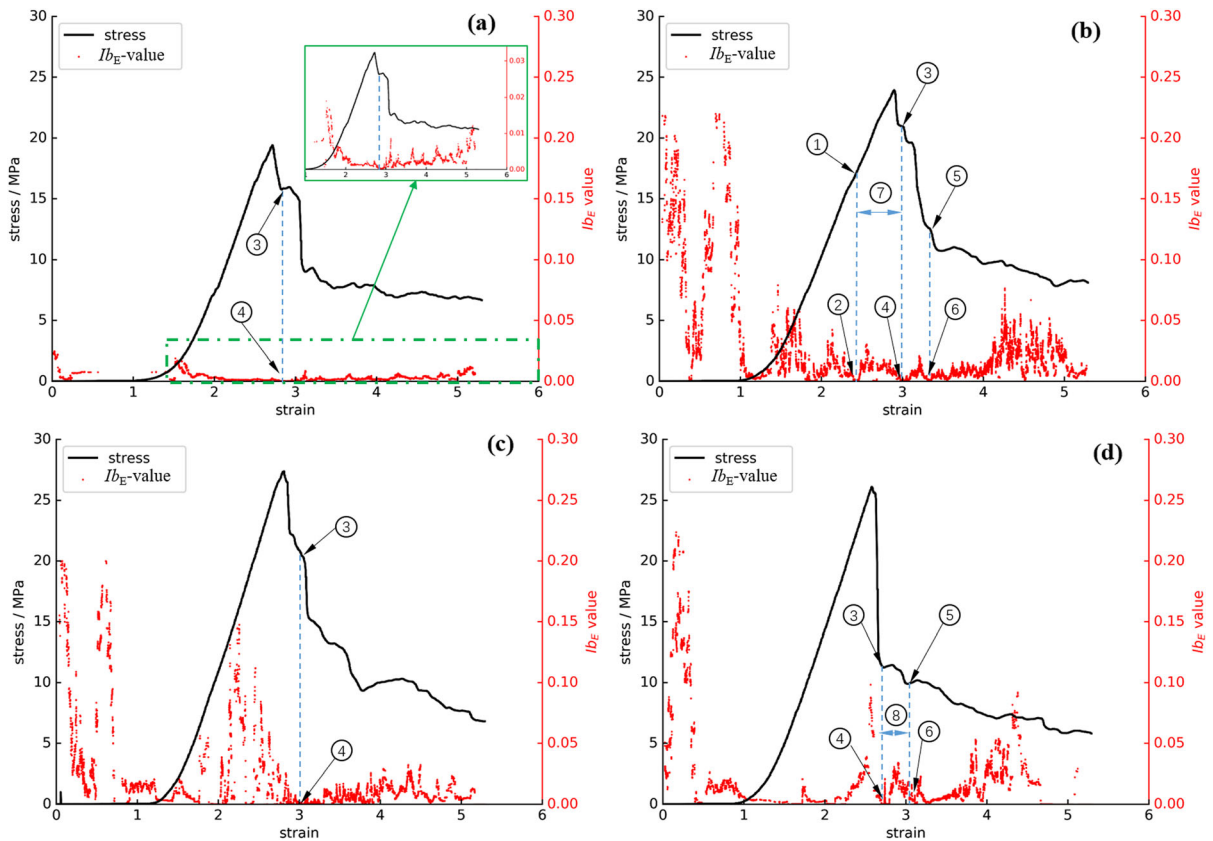


Fig. 6 Ib_E -value characteristics of different brittle rocks during loading. The point ①, ③ and ⑤ are the peak stress point, the first stress drop and the second stress drop in the stress–strain curve,

could be used to measure the size of cracks during rock failure (Rao and Prasanna Lakshmi 2005). Numerous studies have also shown that high ib -values suggest that microcrack initiation in the rock is dominant (Shiotani et al. 2001b, 2003). Some scholars have pointed out that low-energy b -values represent the propagation of macroscopic cracks. When the b_E -value is low, this indicates that the rock interior is undergoing severe damage (Sagasta et al. 2018). Many studies on AE during rock failure have shown that the b_E -value and ib -value have a corresponding relationship with crack propagation in rock (Colombo et al. 2003; Rao and Prasanna Lakshmi 2005). The b -value, ib -value, and ib_E -value are different characterization parameters based on the same principle and therefore have similar corresponding characteristics to the law of rock crack propagation. Therefore, the ib_E -value can also reflect the fracture type. The ib_E is based on the energy change of the AE wave, so the ib_E value is more sensitive to crack propagation. The peak value of

respectively. The point ②, ④ and ⑥ are the corresponding points to ①, ③ and ⑤ on the ib_E curve. The stage of ⑦ and ⑧ are two fracture propagation stage

the ib_E -value indicates that a large number of microcracks have begun to develop in the rock, and the rocks have begun to damage and consume strain energy. The ib_E -value reduction process represents the propagation of cracks, and the cracks expand to its maximum at the lowest ib_E -value. The magnitude of the absolute ib_E -value is not related to the absolute energy of the AE events but is related to the variation in the energy released from the events during the fracture process. The change in the ib_E -value from high to low represents a fracture propagation inside the rock, repeatedly reflected in the continuous pressure drop after the peak (as shown in Fig. 6d).

(2) Analysis of experiment results

Based on the previous analysis, the b_E value change can be used to measure the brittleness of the rock. For example, the ib_E -value drop is evident in the first stress drop after the peak stress in sample 4[#] (in Fig. 6d). Similar situations of ib_E -value drop are also found

during the rock destruction in the other three experiments. Therefore, the crack propagation inside the rock before failure can be judged by the variation characteristics of the ib_E -value, and the decline rate of the ib_E -value determines the brittleness of the rock. The larger the decrease rate of the ib_E -value during rock failure, the greater the brittleness of the rock. The decline rate of the ib_E -value can represent the speed of crack initiation and propagation in the rock, and can be used as an index to describe the brittleness of the rock:

$$BI_{\text{peak}} = (Ib_{E-p} - Ib_{E-r}) / \Delta\varepsilon \quad (3)$$

where Ib_{E-p} is the ib_E -value corresponding to the point of peak stress, Ib_{E-r} is the ib_E -value corresponding to the residual stress, and $\Delta\varepsilon$ represents the strain difference value corresponding to the two ib_E -values.

A sudden drop in the ib_E -value also occurred in the initial loading stage, which indicates that the initial compaction of the rock contains a large amount of micro-crack propagation. With the increase in stress, we found that the ib_E -value of all rocks fluctuated before the peak stress, indicating that the cracks had begun to propagate before peak stress. As shown in Fig. 6b, the stress fluctuation point and its corresponding point of the lowest ib_E value indicate that the interior of the rock experienced a local failure. However, the initiation and propagation of microcracks before the peak is not sufficient to reduce the strength of the rock, and the external stress does not exceed the rock's bearing capacity. As the loading stress increases further, internal micro-cracks develop in large numbers, forming macro cracks, and the rocks produce the first stress drop (Fig. 6b ⊙). For samples 1[#] and 2[#] with weak brittleness, the micro-cracks initiate and propagate before the peak stress, and these crack propagations consume part of the strain energy. The strain energy of the rock is released before the stress peak, which reduces the brittleness of the rock. The internal cracks in these low-brittle rocks begin to expand before the peak, and the pressure drop after the peak of the rock is the final result of crack propagation. For example, in sample 1[#], which had the lowest brittleness, microcrack initiation and propagation began in the rock from the initial loading stage (compaction stage). Several weak crack growths were accompanied in the middle loading stage, which can still be described as a large crack propagation. The entire pre-peak stage of 1[#] sample one can be regarded

as a large crack propagation process. The rate of reduction of the ib_E -value before peak stress was used as an index to evaluate weak, brittle rocks. The specific calculation formula is as follows:

$$BI_{\text{all}} = (Ib_{E-\text{max}} - Ib_{E-\text{min}}) / \Delta\varepsilon \quad (4)$$

where $ib_{E-\text{max}}$ represents the maximum ib_E -value generated during the loading phase, $ib_{E-\text{min}}$ represents the minimum ib_E -value generated after the $ib_{E-\text{max}}$ during the loading phase, and $\Delta\varepsilon$ represents the difference between the two strains.

The BI_{all} distinguishes more significantly against weakly brittle rocks than the BI_{peak} . As shown in Table 1, for rocks with less brittleness (e.g., samples 1[#] and 2[#]), their decline slopes of the ib_E value during the peak pressure drop have one time difference (0.014 and 0.028). The declining slope of the ib_E -value in this stage is used as an index for evaluating low-brittleness rocks, which improves the index difference (0.012 and 0.041) for the two low-brittle samples.

(3) Comparison with Other Evaluation Criteria

Here, we choose the energy brittleness evaluation method (BI_5) of Hucka and Das (1974) and the stress drop brittleness evaluation method (BI_8) of Bishop (1967) to evaluate the brittleness of the samples in this experiment. The energy brittleness evaluation formula is as follows:

$$BI_5 = \frac{U_c}{U_{\text{total}}} \quad (5)$$

where W_{el} indicates the internal elastic energy (the area of CEF in Fig. 7) during rock failure, and W_{tot} represents the work done by the outside world (the area of OABCF in Fig. 7).

The brittleness evaluation method of stress drop is as follows:

$$IB_8 = \frac{\tau_p - \tau_r}{\tau_p} \quad (6)$$

where τ_p represents the shear force at the peak (position C in Fig. 7), and τ_r represents the residual shear stress (position D in Fig. 7).

The evaluation results are compared with the new brittleness indices (BI_{Peak} and BI_{all}) proposed in this paper. The results are shown in Table 3.

The indices of BI_5 and BI_8 are not accurate in evaluating low-brittle rocks. Using the BI_5 method, the brittleness of 3[#] sample three was less than 2[#] sample

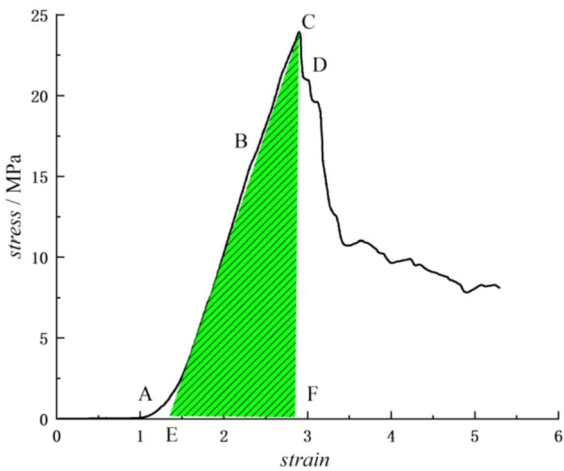


Fig. 7 The relationship between the internal elastic energy of rock and the total loading energy. Area of ABCD and ECF are total loading energy and internal elastic energy, respectively

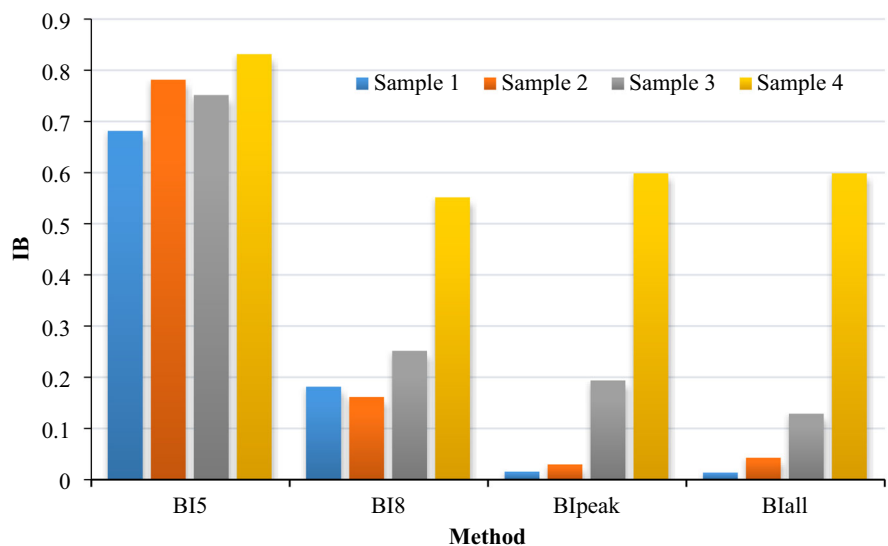
two, while the results of the BI_8 brittleness evaluation method show that the brittleness of 2[#] sample is less

than 1[#] sample one, which is a slight deviation from the actual results. However, the two brittleness evaluation methods proposed in this paper can distinguish the brittleness difference between rocks. At the same time, BI_{peak} and BI_{all} can provide better resolution for different brittle rocks. Most of the energy in brittle rocks are released during the first stress drop. BI_{peak} analyzes the crack propagation process during the stress drop process. Therefore, BI_{peak} accurately evaluates the brittleness of high brittleness rock. Rocks with low brittleness have already released a large amount of energy in the interior before the failure. BI_{all} analyzes the crack propagation process before the stress drop process and can have a more comprehensive evaluation of less brittle rocks. From the evaluation results in Fig. 8, BI_{peak} and BI_{all} have a good resolution for the brittleness of different rocks, and BI_{all} , which considers all stages before the stress peak, has a good resolution for low-brittle rocks. For samples 1[#] and 2[#], BI_{all} and BI_{peak} gave evaluations of

Table 3 Comparison of evaluation results of different brittleness evaluation methods

Specimen	Evaluation result of BI_5	Evaluation result of BI_8	Evaluation result of BI_{peak}	Evaluation result of BI_{all}
1 [#]	0.68	0.18	0.014	0.012
2 [#]	0.78	0.16	0.028	0.041
3 [#]	0.75	0.25	0.192	0.127
4 [#]	0.83	0.55	0.597	0.597

Fig. 8 Comparison of results of different evaluation methods



0.012, 0.041, 0.014, and 0.028, respectively, and BI_{all} had a higher resolution than BI_{peak} in the low brittle region. Both BI_{peak} and BI_{all} 's evaluation resolution for brittle rocks is significantly higher than BI_5 and BI_8 , indicating that the method of evaluating rock brittleness by analyzing AE events can better reflect the nature of rock failure and quantify brittleness more accurately.

4 Conclusion

In this paper, by testing different brittle rock-like materials and using the law of AE events in material fracture, brittleness indexes based on the crack propagation process of the material are proposed. The specific conclusions are as follows:

1. With an increase in rock brittleness, the AE energy gradually shows a sharp increase during rock failure. At the moment of rock failure, the proportion of AE with lower RA and higher AF increases gradually, indicating that tensile cracks increase with brittleness.
2. Based on the Gutenberg and Richter law in earthquakes, combined with the distribution law of AE events energy of rock, an AE index ib_E -value is proposed, reflecting the rock's crack propagation state.
3. The ib_E -value is used to evaluate the brittleness of the rock based on the internal crack propagation law of the rock. A comparison of the existing rock brittleness evaluation methods shows that the evaluation method proposed in this paper is both stable and reliable, and has a higher resolution for the evaluation of different brittle rocks.

Acknowledgments This study was financially supported by the Opening Fund of Key Laboratory of Continental Shale Accumulation and Development (North-east Petroleum University), the National Natural Science Foundation of China (Grant Nos. 42004036, 52074088), Chongqing Science and Technology Commission Projects (Grant Nos. cstc2018jcyj-yszx0005, cstc2020yszx-jcyjX0008). China Postdoctoral Science Foundation (Grant No. 2020M673152).

Declarations

Conflict of interest The authors declare that there is no known conflict of interest. To the best of our knowledge, the named authors have no conflict of interest, financial or otherwise.

References

- Aggelis DG (2011) Classification of cracking mode in concrete by acoustic emission parameters. *Mech Res Commun* 38:153–157. <https://doi.org/10.1016/j.mechrescom.2011.03.007>
- Aggelis DG, Soulioti DV, Barkoula NM et al (2012) Influence of the fiber chemical coating on the fracture behavior of steel fiber concrete measured by acoustic emission. *Emerg Technol Non-Destr Test V* 34:111–115. <https://doi.org/10.1201/b11837-21>
- Bishop AW (1967) Progressive failure—with special reference to the mechanism causing it. In: *Geotechnical Conference*. pp 142–150
- Carpinteri A, Lacidogna G (2006) Structural monitoring and integrity assessment of medieval towers. *J Struct Eng* 132:1681–1690. [https://doi.org/10.1061/\(ASCE\)0733-9445\(2006\)132:11\(1681\)](https://doi.org/10.1061/(ASCE)0733-9445(2006)132:11(1681))
- Chen H, Di Q, Zhang W et al (2021) Effects of bedding orientation on the failure pattern and acoustic emission activity of shale under uniaxial compression. *Geomech Geophys Geo-Energy Geo-Resour*. <https://doi.org/10.1007/s40948-021-00216-x>
- Colombo S, Main IG, Forde MC (2003) Assessing damage of reinforced concrete beam using “b-value” analysis of acoustic emission signals. *J Mater Civ Eng* 15:280–286. [https://doi.org/10.1061/\(ASCE\)0899-1561\(2003\)15:3\(280\)](https://doi.org/10.1061/(ASCE)0899-1561(2003)15:3(280))
- Duan M, Jiang C, Gan Q et al (2020) Experimental investigation on the permeability, acoustic emission and energy dissipation of coal under tiered cyclic unloading. *J Nat Gas Sci Eng* 73:103054–103067. <https://doi.org/10.1016/j.jngse.2019.103054>
- Feng XT, Zhang X, Kong R, Wang G (2016) A novel mogi type true triaxial testing apparatus and its use to obtain complete stress-strain curves of hard rocks. *Rock Mech Rock Eng* 49:1649–1662. <https://doi.org/10.1007/s00603-015-0875-y>
- Garcimartín A, Guarino A, Bellon L, Ciliberto S (1997) Statistical properties of fracture precursors. *Phys Rev Lett* 79:3202–3205. <https://doi.org/10.1103/PhysRevLett.79.3202>
- Gong F, Yan J, Li X (2018) A new criterion of rock burst proneness based on the linear energy storage law and the residual elastic energy index. *Yanshilixue Yu Gongcheng Xuebao/Chin J Rock Mech Eng*. <https://doi.org/10.13722/j.cnki.jrme.2018.0232>
- Gong F, Yan J, Luo S, Li X (2019) Investigation on the linear energy storage and dissipation laws of rock materials under uniaxial compression. *Rock Mech Rock Eng*. <https://doi.org/10.1007/s00603-019-01842-4>
- Grieser B, Bray J (2007) Identification of production potential in unconventional reservoirs. In: *SPE production and operations symposium, proceedings. society of petroleum engineers*, pp 243–248
- Grosse CU, Ohtsu M (2008) *Acoustic emission testing: basics for research-applications in civil engineering*. Springer, Heidelberg

- Gutenberg B, Richter CF (1945) Frequency of earthquakes in California. *Nature* 156:371. <https://doi.org/10.1038/156371a0>
- Hirata T (1987) Omori's power law aftershock sequences of microfracturing in rock fracture experiment. *J Geophys Res* 92:6215–6221. <https://doi.org/10.1029/JB092iB07p06215>
- Hucka V, Das B (1974) Brittleness determination of rocks by different methods. *Int J Rock Mech Min Sci Geomech Abstr* 11:389–392
- Jahandideh A, Jafarpour B (2016) Optimization of hydraulic fracturing design under spatially variable shale fracability. *Soc Pet Eng SPE West N Am Rocky Mt Jt Meet* 138:174–188. <https://doi.org/10.2118/169521-ms>
- Jarvie DM, Hill RJ, Ruble TE, Pollastro RM (2007) Unconventional shale-gas systems: the Mississippian Barnett Shale of north-central Texas as one model for thermogenic shale-gas assessment. *Am Assoc Pet Geol Bull.* <https://doi.org/10.1306/121906060608>
- Kurz JH, Finck F, Grosse CU, Reinhardt HW (2006) Stress drop and stress redistribution in concrete quantified over time by the b-value analysis. *Struct Heal Monit* 5:69–81. <https://doi.org/10.1177/1475921706057983>
- Li Y, Yang S, Zhao W et al (2018) Experimental of hydraulic fracture propagation using fixed-point multistage fracturing in a vertical well in tight sandstone reservoir. *J Pet Sci Eng* 171:704–713. <https://doi.org/10.1016/j.petrol.2018.07.080>
- Li H, Dong Z, Ouyang Z et al (2019a) Experimental investigation on the deformability, ultrasonic wave propagation, and acoustic emission of rock salt under triaxial compression. *Appl Sci* 9:635–650. <https://doi.org/10.3390/app9040635>
- Li Y, Cai W, Li X et al (2019b) Experimental and DEM analysis on secondary crack types of rock-like material containing multiple flaws under uniaxial compression. *Appl Sci* 9:1749–1765. <https://doi.org/10.3390/app9091749>
- Li Y, Long M, Zuo L et al (2019c) Brittleness evaluation of coal based on statistical damage and energy evolution theory. *J Pet Sci Eng* 172:753–763. <https://doi.org/10.1016/j.petrol.2018.08.069>
- Lin Q, Mao D, Wang S, Li S (2018) The influences of mode II loading on fracture process in rock using acoustic emission energy. *Eng Fract Mech* 194:136–144. <https://doi.org/10.1016/j.engfracmech.2018.03.001>
- Mansurov VA (1994) Acoustic emission from failing rock behaviour. *Rock Mech Rock Eng* 27:173–182. <https://doi.org/10.1007/BF01020309>
- Munoz H, Taheri A, Chanda EK (2016a) Fracture energy-based brittleness index development and brittleness quantification by pre-peak strength parameters in rock uniaxial compression. *Rock Mech Rock Eng.* <https://doi.org/10.1007/s00603-016-1071-4>
- Munoz H, Taheri A, Chanda EK (2016b) Fracture energy-based brittleness index development and brittleness quantification by pre-peak strength parameters in rock uniaxial compression. *Rock Mech Rock Eng* 49:4587–4606. <https://doi.org/10.1007/s00603-016-1071-4>
- Ohtsu MTY (2011) Phenomenological model of corrosion process in reinforced concrete identified by AE. *Concr Res Lett* 2:280–285
- Parney R, Lange N (2010) Comparison of seismic brittleness and anisotropy to micro-seismic in the Waltman Shale. In: Society of exploration geophysicists international exposition and 80th annual meeting 2010, SEG 2010. Society of Exploration Geophysicists, pp 278–282
- Perez R, Marfurt K (2013) Brittleness estimation from seismic measurements in unconventional reservoirs: application to the Barnett shale. In: Society of exploration geophysicists international exposition and 83rd annual meeting, SEG 2013: expanding geophysical frontiers. Society of Exploration Geophysicists, pp 2258–2263
- Rao MVMS, Prasanna Lakshmi KJ (2005) Analysis of b-value and improved b-value of acoustic emissions accompanying rock fracture. *Curr Sci* 89:1577–1582
- Rickman R, Mullen M, Petre E, et al (2008) A practical use of shale petrophysics for stimulation design optimization: all shale plays are not clones of the Barnett Shale. In: Proceedings—SPE annual technical conference and exhibition. pp 840–850
- Sagasta F, Zitto ME, Piotrkowski R et al (2018) Acoustic emission energy b-value for local damage evaluation in reinforced concrete structures subjected to seismic loadings. *Mech Syst Signal Process* 102:262–277. <https://doi.org/10.1016/j.ymssp.2017.09.022>
- Schiavi A, Niccolini G, Tarizzo P et al (2011) Acoustic emissions at high and low frequencies during compression tests in brittle materials. *Strain* 47:105–110. <https://doi.org/10.1111/j.1475-1305.2010.00745.x>
- Shiotani T, Bisschop J, Van Mier JGM (2003) Temporal and spatial development of drying shrinkage cracking in cement-based materials. *Eng Fract Mech* 70:1509–1525. [https://doi.org/10.1016/S0013-7944\(02\)00150-9](https://doi.org/10.1016/S0013-7944(02)00150-9)
- Shiotani T, Fujii K, Aoki T, Amou K (1994) Evaluation of progressive failure using AE sources/Improved b-value on slope model tests. *Prog Acoust Emiss VII*:529–534
- Shiotani T, Ohtsu M, Ikeda K (2001a) Detection and evaluation of AE waves due to rock deformation. *Constr Build Mater* 15:235–246. [https://doi.org/10.1016/S0950-0618\(00\)00073-8](https://doi.org/10.1016/S0950-0618(00)00073-8)
- Shiotani T, Yuyama S, Li ZW, Ohtsu M (2001b) Application of AE improved b-value to quantitative evaluation of fracture process in concrete materials. *J Acoust Emiss* 19:118–133
- Song ZL, Han PB, Li WP et al (2015) Impact of energy dissipation of coal samples with rockburst tendency from gas in its failure process. *Meitan Xuebao/J China Coal Soc* 40:843–849. <https://doi.org/10.13225/j.cnki.jccs.2014.3019>
- Stankevych O, Skalsky V (2016) Investigation and identification of fracture types of structural materials by means of acoustic emission analysis. *Eng Fract Mech* 164:24–34. <https://doi.org/10.1016/j.engfracmech.2016.08.005>
- Tarasov B, Potvin Y (2013) Universal criteria for rock brittleness estimation under triaxial compression. *Int J Rock Mech Min Sci.* <https://doi.org/10.1016/j.ijrmms.2012.12.011>
- Turcotte DL, Newman WI, Shcherbakov R (2003) Micro and macroscopic models of rock fracture. *Geophys J Int* 152:718–728. <https://doi.org/10.1046/j.1365-246X.2003.01884.x>
- Wang FP, Gale JFW (2009) Screening criteria for shale-gas systems. *Gulf Coast Assoc Geol Soc Trans*

- Wang T, Zhang H, Gamage RP et al (2020) The evaluation criteria for rock brittleness based on double-body analysis under uniaxial compression. *Geomech Geophys Geo-Energy Geo-Resour* 6:1–19
- Wanniarachchi WAM, Ranjith PG, Perera MSA et al (2015) Current opinions on foam-based hydro-fracturing in deep geological reservoirs. *Geomech Geophys Geo-Energy Geo-Resour* 1:121–134. <https://doi.org/10.1007/s40948-015-0015-x>
- Watanabe T, Nishibata S, Hashimoto C, Ohtsu M (2007) Compressive failure in concrete of recycled aggregate by acoustic emission. *Constr Build Mater* 21:470–476. <https://doi.org/10.1016/j.conbuildmat.2006.04.002>
- Yang J, Yang SQ, Liu GJ et al (2021) Experimental study of crack evolution in prefabricated double-fissure red sandstone based on acoustic emission location. *Geomech Geophys Geo-Energy Geo-Resour*. <https://doi.org/10.1007/s40948-021-00219-8>
- Yang W, Li G, Ranjith PG, Fang L (2019) An experimental study of mechanical behavior of brittle rock-like specimens with multi-non-persistent joints under uniaxial compression and damage analysis. *Int J Damage Mech* 28:1490–1522. <https://doi.org/10.1177/1056789519832651>
- Zhang D, Ranjith PG, Perera MSA (2016) The brittleness indices used in rock mechanics and their application in shale hydraulic fracturing: a review. *J Pet Sci Eng* 143:158–170. <https://doi.org/10.1016/j.petrol.2016.02.011>
- Zhang Dm, Yang Ys, Yang H et al (2018a) Experimental study on the effect of high temperature on the mechanical properties and acoustic emission characteristics of gritstone. *Results Phys* 9:1609–1617. <https://doi.org/10.1016/j.rinp.2018.05.013>
- Zhang J, Ai C, Li Yw et al (2018b) Energy-based brittleness index and acoustic emission characteristics of anisotropic coal under triaxial stress condition. *Rock Mech Rock Eng*. <https://doi.org/10.1007/s00603-018-1535-9>

Publisher's Note Springer Nature remains neutral with regard to jurisdictional claims in published maps and institutional affiliations.